SYNTHESIS OF CONTROLLED LAYERS OF POLY(ACRYLIC ACID) AND THEIR INTERACTION WITH AMINOFUNCTIONAL SILSESQUIOXANE NANOPARTICLES

Markus Retsch[a], Andreas Walther[a], Katja Loos[b], Axel H. E. Müller[a]

[a]Makromolekulare Chemie II, Universität Bayreuth, 95440 Bayreuth, Germany; e-mail: axel.mueller@uni-bayreuth.de
[b]Department of Polymer Chemistry, Materials Science Centre, University of Groningen, 9747AG Groningen, The Netherlands

Introduction

Over the last decade the development of nanotechnology has become increasingly important. The surface of objects in the nanometre scale plays a major role since their properties are governed by their huge interface. Controlling the surface properties of any material in the nanometre range is the linchpin to adjust its properties and its interaction potential.

Polymer brushes (a layer consisting of polymer chains dangling in a solvent with one end attached to a surface is frequently referred to as a polymer brush) offer excellent possibilities to tailor surface properties. Two methods are commonly used to obtain polymer brushes, "grafting to" and "grafting from". The former attaches pre-built polymers by reactive end- or sidegroups to functional surfaces yielding thin layers of low grafting density. The latter grows the polymer brushes **from** a surface covered with an initiator species and is the superior alternative as the functionality, density and thickness of the polymer brushes can be controlled with almost molecular precision.

The use of polyelectrolyte brushes results in a class of materials with highly interesting behaviour due to their high electrostatic potential within the layer. Their properties can be switched by external stimuli like pH, ionic strength or temperature.[1] This behaviour can be utilized for the formation of adjustable hybrid complexes and architectures with for instance inorganic nanoparticles.

Here we report on the synthesis of poly(acrylic acid) polyelectrolyte brushes on gold surfaces and on first studies on their interaction with nanoparticles.

Experimental

Materials. (5'-Trichlorosilylpentyl) 2-bromo-2-methylproprionate[2] (**a**) and 11-mercaptoundecyl-(2-bromo 2-methyl)propionate[3] (**b**) were synthesized according to literature and are shown in **Scheme 1**.

Scheme 1

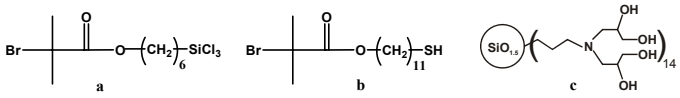

The silica nanoparticles (**Scheme 1, c**) were synthesized according to literature.[4] They have a diameter of ~ 3 nm, a molecular weight of ~ 3760 g/mol and bear about 14 amino functions per core.

Monolayer Formation. Three different kinds of self-assembled monolayers (SAM) were produced and will be denoted as Monopod (**d**), Tripod (**e**) and Crosslinked SAM (**f**) in the following. Freshly produced gold surfaces on glass or silicon substrates (with an intermediate layer of chromium for better adhesion of the gold) were used in all cases.

Monopod Monolayer (**d**): The gold surfaces were submerged in a weighing glass into a solution of 13 mg of **b** in 20 ml of EtOH (HPLC grade, ~ 2 mM). The weighing glass was set under Argon and formation of the SAM was allowed for five days. Afterwards the substrates were extensively washed with EtOH p.a. and dried in a stream of N_2.

Tripod Monolayer (**e**): The gold surfaces were immersed in a solution of 9.2 mg of 3-mercapto propanol in 50 ml of EtOH (HPLC grade). SAM formation was allowed for 8 days. Afterwards the surfaces were washed extensively with EtOH and the dried substrates were stored under argon.

For the attachment of the ATRP-Initiator the 3-mercapto propanol SAM's were covered with a layer of 5 ml dry toluene to which 0.5 ml of **a** were added. Finally 0.5 ml of triethylamine was added drop wise. The flask was kept under argon and was gently shaken for one hour. Finally the substrates were washed with copious amounts of MeOH and dichloromethane. The substrates were stored in dichloromethane and blown dry with N_2 prior to use.[2]

Crosslinked SAM (**f**): The gold substrates were incubated in a solution of 21.1 mg 3-mercaptopropyl trimethoxysilane in 25 ml of dry MeOH (~ 4 mM). The SAM formation was allowed to proceed for 6.5 h. Subsequently the substrate was immersed into a 0.1 M HCl solution for 4.5 h to crosslink the immobilized trimethoxy silane groups via a sol-gel process. After that the substrates were rinsed with pure water and dried with nitrogen.[5]

The immobilization of the ATRP-Initiator was conducted in a glove box. The 3-mercaptopropyl trimethoxysilane SAM's were submerged into a solution of 0.4 ml of **a** in 6 ml of dry toluene. Triethylamine (0.31 ml) was dispersed in 4 ml of dry toluene and was added slowly and evenly over the entire solution in the weighing dish. The reaction was allowed to proceed for 4 h. Finally the substrates were immersed into 6 ml dichloromethane and rinsed twice with MeOH and stored under dichloromethane. Prior to use they were blown dry with N_2.[2]

Surface Initiated Polymerization. The reaction mixture was typically weighed in a glove box. 27.3 mg (0.73 mmol) of N,N,N',N'',N''-pentamethyldiethylenetriamine, 24.4733 g (0.19 mol) of *tert*-butyl acrylate and 70.2 mg (0.489 mmol) of CuBr were weighed into a 50 ml screw-thread bottle. After the CuBr was dissolved 0.824 mg (7.62 mmol) anisole and 15.6551 g (0.270 mol) of acetone were added. After the solution was stirred for another five minutes 47.7 mg (0.2448 mmol) ethyl 2-bromoisobutyrate were added. The clear, light greenish solution was well stirred and finally dispersed on ca. 10 ml screwthread round bottom flasks, which contained the initiator immobilized surfaces **d**, **e** or **f** respectively. Approximately 3.5 ml polymerization mixture was used for each substrate. The flasks were sealed with a rubber septum, which allowed taking samples throughout the polymerization.[6]

The polymerization was conducted at a temperature of 60°C. Samples were repeatedly taken during the reaction to measure the conversion. The polymerization was stopped by addition of dichloromethane, THF and exposure to air. The substrates were rinsed with copious amounts of THF p.a. To remove any adsorbed polymer on the grafted layer, the substrates were subjected to Soxhlet extraction in THF for at least six hours.

The free polymer generated by sacrificial initiator in the solution was passed through a silica gel column to remove the copper catalyst and was analyzed by GPC.

Hydrolysis of Poly(*tert*-butylacrylate) Brushes. 100 µl of methanesulfonic acid ($MeSO_3H$) were dissolved in 10 ml of dichloromethane.[7] The Poly(*tert*-butyl acrylate) grafted samples were immersed for a period of 60 seconds. Afterwards the substrates were immediately rinsed with copious amounts of EtOH and dried in a stream of nitrogen.

Results and Discussion

Monolayer Formation. Three types of monolayers were synthesized, which varied in the number of binding sites to the gold surface per initiating moiety. These three different architectures are sketched in **Scheme 2** and will be referred to as Monopod SAM (**d**), Tripod SAM (**e**) and Crosslinked SAM (**f**).

Scheme 2

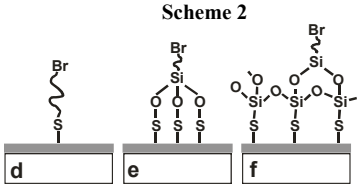

The successful formation of each SAM was monitored by Phase Modulation – Infrared Reflection Absorption Spectroscopy (PM-IRRAS), X-ray Photoelectron Spectroscopy (XPS) and water contact angle measurements.

The typical water contact angle evolution throughout the course of surface functionalization steps (in the case of the crosslinked SAM **f**) is shown in **Figure 1**.

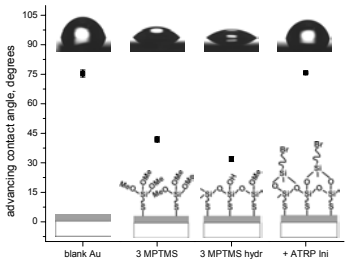

Figure 1. Water contact angle evolution during crosslinked monolayer formation.

The initial water contact angle for pure gold was repeatedly measured to be around 75°, which derives from adsorption of hydrophobic molecules from the atmosphere to the highly reactive gold surface. Upon deposition of 3-MPTMS the surface becomes more hydrophilic, which leads to a contact angle of about 42°. After hydrolysis the contact angle drops further to 32°, which originates from the cleavage of the methoxy-groups. Deposition of the ATRP α-bromoester initiator **a** results in a more hydrophobic surface with a contact angle of 76°. Analogous results were obtained for all samples.

The successful formation of all monolayers was confirmed by XPS measurements.

The result of PM-IRRAS measurements of the Monopod SAM system (**d**) are shown in **Figure 2**.

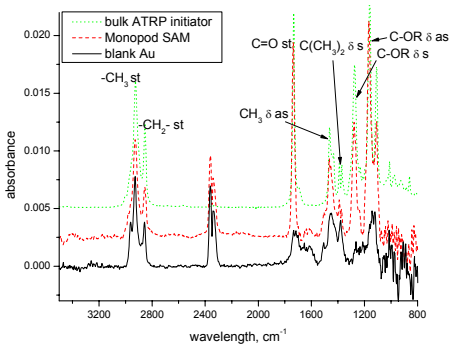

Figure 2. PM-IRRAS analysis of the Monopod monolayer formation.

PM-IRRAS proves the formation of a dense layer of the ATRP initiator, since the spectra of the bulk and the surface-immobilized initiator match each other. The position of the methylene peaks indicate a rather disorderd state of the molecules in the monolayer according to Porter et al.[8] In case of the Tripod and Crosslinked monolayer the successful deposition could be observed by the appearance of Si-O and C=O stretching modes.

Surface-Initiated Polymerization. The same polymerization conditions were applied to all three types of substrates. The layer thickness of the grafted brush was adjusted by quenching at different stages of conversion. The kinetics of polymerization on the substrate and in solution was found to be the same. Therefore it can be concluded that the grafted and free polymer chains have the same degree of polymerization. GPC results of the free polymer showed that very narrowly dispersed polymers with a PDI < 1.1 were obtained in most cases. For all three types of monolayers a linear dependence between degree of polymerization and layer thickness was found. The layer thickness was determined by ellipsometry and homogeneous layers of polymer brushes were found. The average grafting density of each type of substrate was calculated on the basis of at least six samples of various layer thicknesses. The average grafting densities for Monopod (**d**), Tripod (**e**) and Crosslinked SAM (**f**) were found to be 0.37 ± 0.02, 0.47 ± 0.04 and 0.39 ± 0.04 chains/nm^2, respectively. Thus the type of the monolayer has only a minor influence on the grafting density. The acidic hydrolysis of the *tert*-butyl group turned out to depend strongly on the type of underlying monolayer, the result is given in **Figure 3**.[7]

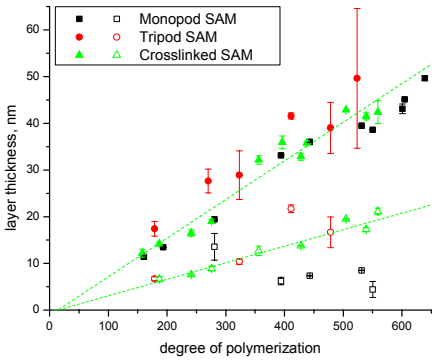

Figure 3. Layer thickness of the grafted polymer film before and after hydrolysis in dependence of the degree of polymerization. Filled symbols indicate PtBA brushes, open symbols show the remaining layer after hydrolysis. The straight lines are linear fits to the Crosslinked SAM **f**.

Figure 3 shows that the Tripod (**e**) and Crosslinked (**f**) monolayers are stable enough to tolerate the acidic hydrolysis with methanesulfonic acid. In both cases the layer thickness decreased reproducibly by about 57% for each sample. In case of the Monopod monolayer (**d**) an irregular and much larger degree of shrinkage was found, which might originate from polymer chains that are cleaved away from the substrate during hydrolysis.

Adsorption of Silsesquioxane Nanoparticles into the Poly(acrylic acid) Brushes. The crosslinked SAM substrates (**f**) were chosen to evaluate the interaction of the polyelectrolyte brushes with silsesquioxane nanoparticles. pH dependent adsorption of the nanoparticles into and onto the brushes was followed by surface plasmon resonance (SPR) experiments. For that purpose 80 µl of pH adjusted nanoparticle solution were repeatedly injected onto the brush surfaces. The residual increase in SPR signal after rinsing with a nanoparticle-free solution of the same pH is a direct measure for the amount of adsorbed particles. The pH was varied from pH 3.0 to 8.0. It was found that a maximum adsorption was achieved at a pH of roughly 5.3. Recovery of the bare polyelectrolyte brush was performed by injection of 0.1 M HCl solution.

Layer-by-Layer Architecture with Silica Nanoparticles. Layer-by-Layer architecture construction of silica nanoparticles and PAA was attempted at the maximum interaction pH of 5.3 and also followed by SPR, **Figure 4**.

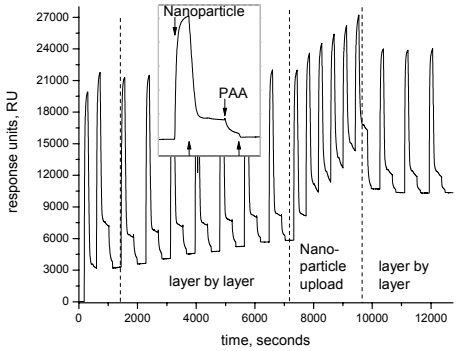

Figure 4. LBL on a 16.1 nm layer of PAA-brush at a pH of 5.3 as seen by SPR. Inset: Downward pointing arrows indicate start of injection, upward pointing arrows show the end of injection.

The repeated and alternating injection of nanoparticles and PAA led to a slight increase in the SPR signal; however this turned out not to be caused by a LBL architecture but rather by a very slow uptake of nanoparticles into the brush. No further increase in the SPR signal can be detected during the repeated cycles of nanoparticle and PAA injection after the brush was fully loaded with nanoparticles. Thus one has to conclude that at that point an equilibrium was reached at which slightly bound particles are washed away due to interaction with the subsequently injected PAA. In the early stages (the brush is not fully loaded) a certain amount of nanoparticles becomes tightly bound to or within the brush and can not be washed away by the ensuing PAA, which causes the SPR signal to increase slightly with each cycle of injection.

Conclusions

Highly uniform and homogenous brushes of PAA were synthesized on planar gold surfaces. The binding strength of the SAM to the gold surface is of crucial importance to reproducibly hydrolyse the *tert*-butyl moieties of the grafted polymer. It turned out that Tripod and Crosslinked monolayers are suitable for that purpose; they yield polymer brushes with high grafting density and are stable enough to sustain acidic hydrolysis. The PtBA layers shrink upon hydrolysis by about 57%.

The pH dependent interaction of the PAA brushes with nanoparticles was found to be maximum at a pH of about 5.3. An attempt was undertaken to build up LBL structures of silica nanoparticles and PAA above these PAA brushes. It turned out that no LBL structures were formed; the nanoparticles rather penetrated the PAA brushes.

Acknowledgements. This research was funded by DFG. The authors thank Joachim E. Klee (Dentsply DeTrey) for the nanoparticle synthesis and Prof. P. Rudolf and the group of Surfaces and Thin Films (Materials Science Centre) for access to the X-ray photoelectron spectrometer.

References

(1) Rühe, J.; Ballauff, M.; Biesalski, M.; Dziekok, P.; Gröhn, F.; Johannsmann, D.; Houbenov, N.; Hugenberg, N.; Konradi, R.; Minko, S.; Motornov, M.; Netz, R. R.; Schmidt, M.; Seidel, C.; Stamm, M.; Stephan, T.; Usov, D.; Zhang, H. *Adv Polym Sci* **2004,** 165, 79-150.
(2) Husseman, M.; Malmström, E. E.; McNamara, M.; Mate, M.; Mecerreyes, D.; Benoit, D. G.; Hedrick, J. L.; Mansky, P.; Huang, E.; Russell, T. P.; Hawker, C. J. *Macromolecules* **1999,** 32, (5), 1424-1431.
(3) Jones, D. M.; Brown, A. A.; Huck, W. T. S. *Langmuir* **2002,** 18, 1265
(4) Mori, H.; Lanzendorfer, M. G.; Müller, A. H. E.; Klee, J. E. *Macromolecules* **2004,** 37, (14), 5228-5238
(5) Kambhampati, D. K.; Jakob, T. A. M.; Robertson, J. W.; Cai, M.; Pemberton, J. E.; Knoll, W. *Langmuir* **2001,** 17, 1169-1175.
(6) Treat, N. D.; Ayres, N.; Boyes, S. G.; Brittain, W. J. *Macromolecules* **2006,** 39, 26-29.
(7) Dai, J.; Bao, Z.; Sun, L.; Hong, S. U.; Baker, G. L.; Bruening, M. L. *Langmuir* **2006,** 22, 4274-4281.
(8) Porter, M. D.; Bright, T. B.; Allara, D. L.; Chidseyi, C. E. D. *J. Am. Chem. Soc.* **1987,** 109, 3559-3568.